ISSN: 0975-833X

Available online at http://www.journalcra.com

International Journal of Current Research
Vol. 17, Issue, 10, pp.34885-34889, October, 2025
DOI: https://doi.org/10.24941/ijcr.49523.10.2025

INTERNATIONAL JOURNAL OF CURRENT RESEARCH

RESEARCH ARTICLE

ELECTRODE ARRANGEMENT OPTIMIZATION OF AIR ATMOSPHERIC CORONA DISCHARGE IN PLATE-LINE-PLATE CONFIGURATION

Won-Jun Kim, Yong-Son Choe, *Yong-Jun Kim and Kwang-Won Cha

Faculty of Physical Engineering, Kim Chaek University of Technology, Pyongyang, Democratic People's Republic of Korea

ARTICLE INFO

Article History:
Received 24th July, 2025
Received in revised form
25th August, 2025
Accepted 17th September, 2025
Published online 30th October, 2025

Keywords:

Atmospheric Corona Discharge, Electric Field, Electrode Arrangement, Optimization.

***Corresponding author:** *Yong-Jun Kim*

ABSTRACT

It is important to find the optimized electrode arrangement in the atmospheric corona discharge for various applications such as harmful gas removal. The line-line and line-plane distances were investigated for plate-line-plate configuration by simulation and experiment of electric field distribution of the atmospheric corona discharge. The applied voltages varied 1 to 10 kV while the distances were adjusted 10 to 40mm. COMSOL Multiphysics simulation and experiment results showed that the line-line distance of 34 to 40mm results in more homogeneous and high electric field distribution for the corona discharge. When the ratio between line-line and line-plate distances is 1.7 to 2 at a constant applied voltage, the highest current density could be reached.

Citation: Won-Jun Kim, Yong-Son Choe, Yong-Jun Kim and Kwang-Won Cha. 2025. "Electrode arrangement optimization of air atmospheric corona discharge in plate-line-plate configuration". *International Journal of Current Research, 17, (10), 34885-34889.*

INTRODUCTION

Atmospheric discharge technology, which produces non-equilibrium plasma in air, has been utilized for various industrial applications including cleaning of indoor air and sewage, ozone generation, and so on (Fukui *et al*., 2015; Zheng *et al*., 2010; Cheng *et al*., 2012; Pien, 2020; Dai *et al*., 2024; Leng *et al*., 2021; Wang *et al*., 2020; Liu, 2021; Arcanjo, 2021). Although there are many advanced reports on the atmospheric discharge plasma, the stabilized, controlled and homogenous atmospheric plasma is still open and requires further investigation. The typical electrode configurations include coaxial cylinders, needle-plane, and line-plane. However, it was reported that the plate-line-plate (PLP) would be more effective for some applications such as harmful gas removal (Rong, 2016; Michael, 2003). The PLP atmospheric corona discharge depends on many factors: line-line distance, line-plane distance, line diameter, applied voltage, current intensity, gas flow rate, and so on (Rong, 2016; Zakari, 2015). Many efforts have been devoted to simulations and experiments of atmospheric corona discharges. Most of them were, however, limited to the influence of charged particles drift on the discharge current intensity (Toshiaki, 2025, 5**),** or the effect of space charges on the electrical field distribution (Zheng *et al*., 2010; Paria, 2011). Some reports can be found that atmospheric corona discharge structures were analyzed by software tool FLUENT and compared to the experiment measurements (Paria, 2011; Zhao, 2008). They utilized Immersed Boundary Method (IBM), FEM, and FCT to investigate atmospheric corona discharge characteristics of different electrode configurations such as cylinder-plane and needle-plane (Kenneth, 2006; Papageorgiou, 2011; Papageorgiou, 2011; Breden, 2012; Benkhaldoun, 2012). It was also reported that dielectric barrier discharges (DBD) could be analyzed for non-steady state by considering generation and extinction of various species (Sato *et al*., 2019; Tanaka *et al*., 2016; Payen *et al*., 2011; Wang, 2011; Bahaeva, 2010). They combined CFD method with FEM or FDM to enhance the analysis accuracy of complex discharge geometry (Fukui, 2015; Shao, 2011). Recently, plasma flow equations, which are based on the plasma fluid modeling (PFM), were applied to the atmospheric low temperature plasma ejection (Zakari *et al*., 2015; Cheng *et al*., 2012). They combined gas flow models (GFM) and discharge models to give hydrodynamical descriptions to the motion of discharged and neutral species. Although the above methods are accepted effective in some cases, a more comprehensive method is needed for the complicated applications such as air pollutant removal. The performance of PLP corona discharge is dependent on many parameters: gas flow rate, voltage, current, and shape, size, and arrangement of electrodes (Michael, 2003). Such requirements permit us to utilize the well-built software tool COMSOL Mutiphysics for our research.We aim to find the suitable line-plane and line-line distances for homogeneous and high electric field through 3D simulations and experiments. And we estimate potential distribution, species concentration, current density at the optimized electrode arrangement.

MODELING

Geometry: The cross section of PLP corona geometry is shown in Figure 1. Several line electrodes are placed at the mid between the two plate electrodes. And the line electrodes are equally spaced parallel to the plate electrodes. The PLP geometry is characterized by the line-plate distance, line-line distance, line radius, parallel-to-plate

length, normal-to-plate width, and number of lines. The working gas, air, enters the discharge region from the left and exits to the right.

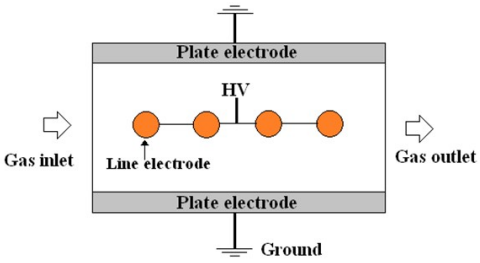

Figure 1. Cross section of plane-line-plane corona discharge geometry

Physical modeling: The corona discharge is modeled based on the plasma fluid model (PFM), which includes the drift-diffusion equations of plasma species and Poisson equation. All the equations come from COMSOL Multiphysics default equations. All the bulk reactions are listed in table 1, where *A* denotes air molecule, *e* designates electron, *n* means negative ion, and *p* stands for positive ion. It is assumed that single-valued ions are only possible due to the non-equilibrium consideration and all the ions are incorporated into negative ion *n* and positive ion *p* regardless of their ionization states.

In the Table 1, N_A, T_e and T_0 denote Avogadro constant, electron temperature, gas temperature. All the necessary parameters are listed in the Table 2 with their considered ranges. The air is regarded as ideal gas and our case is the negative corona discharge.

RESULTS AND DISCUSSION

Electric field: Figure 2 shows electric field distribution for different line eletrode arrangements, where applied voltage is 8kV and line diameter is 0.2mm. It can be seen that the narrow regions with high electric field forms around line electrodes, which is typical of corona discharge (Zheng *et al*., 2010; Michael, 2003). In particular, the more line electrodes results in lower peak electric field, but enlarges the corona regions around the line electrodes. The fact permits us to vary the geometry parameters such as line diameter, line-line distance, and line-plate distance.

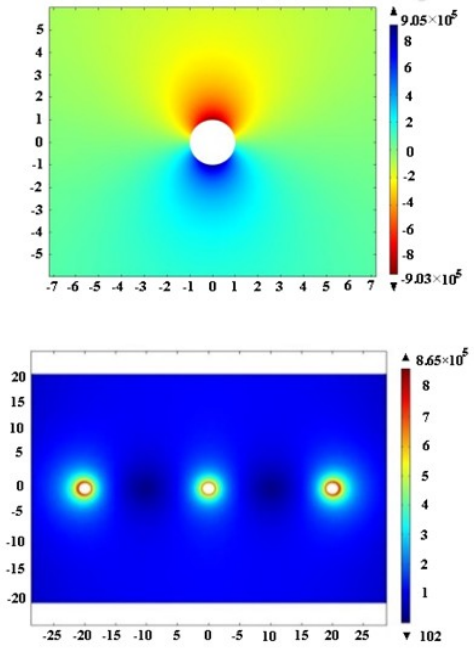

Figure 2. Distribution of electric field with one line electrode(left) and absolute electric field with three line electrodes(right): applied voltage 8kV and line diameter 0.2mm

Therfore we simulated the PLP corona discharge by varying the line diameter from 0.05 to 0.3mm, line-line distance from 10 to 40mm, and line-plate distance from 10 to 30mm.

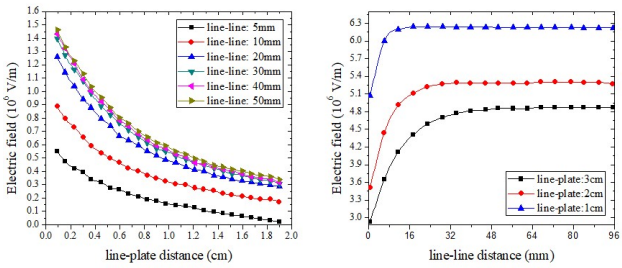

Figure 3. Variation of peak electric field with line-plane distance (left) and line-line distance (right): the line diameter 0.2 mm, voltage 8kV

Figure 3 presents the variation of peak electric field with line-line distance and line-plate distance when applied voltage is 8kV and line diameter is 0.02mm. The peak electric field decreases with all the line-plate distances due to the constant applied voltage. Meanwhile, the line-plate distance above 30mm lead to no significant variation of peak electric field. And the peak electric field saturates with line-line distance because the influence of neighbour line electrodes decreases to the case of an isolated line electrode. Especicially, when line-plate distance is changed from 1cm to 2cm, the peak field declines substantially. In all cases, the peak electric field does not exceed 6.3×10^6V/m. This fact allows us to perfer the line-line distance smaller than 40mm and the line-plate distance lower than 2cm for the PLP corona discharge.

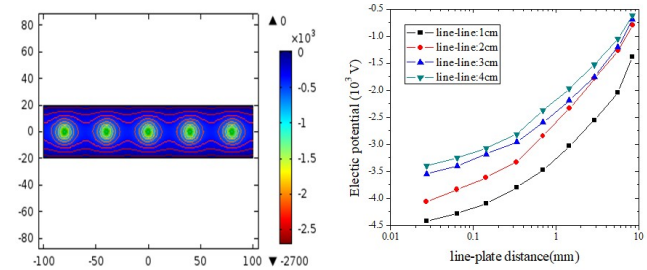

Figure 4. Potential contours around line electrodes(left) and inter-line average potential with line-plate gap (right)

Figure 4 shows the potential contours around line electordes and average potetial at the mid between the line electrodes. As the line diameter is so narrow, much of potential drop appears in the corona region around the line electrode. It can be seen that the inter-line arverage potential grows with the line-plate distance but decreases with the line-line distance. When the line-line distance is greater than 3cm, the effect of line-plate appears to be ignored. And the line-plate distance less than 1cm gives rise to relatively uniform average potential, which can reach half the applied voltage. This fact confirms that we should have an optimized line-line to line-plate distance ratio to produce a large corona region with high electric field.

Electric potential: In order to have a large corona region with high electric field, the electric potential distribution should be investigated. Figure 5 illustrates the potential distribution around the line electrodes with different line-line distance. The simulation conditions are as follows: applied voltage 8kV; line diameter 0.2 mm; line-plate distance 2cm; number of lines 5. As expected, the lower the line-line distance gets, the larger corona region forms. It is interesting to say that the corona regions of individual line electrode merge into an oval form at the line-line distance of 10mm, while the corona regions merge partially or separate from one another in the other cases. It reflects that the line-line distance should be less than 20mm for a large corona region of PLP corona discharge. In our case, we set the threshold potential for corona region to 2kV, which is 25% of the applied voltage, 8kV.

Table 1. Bulk reactions of air

Reaction	Rate coefficient	Type	Energy	Reference
$A+e \rightarrow p+2e$	Townsend coefficient	ionization	15 eV	COMSOL
$A+e \rightarrow n$	Townsend coefficient	recombination	-	COMSOL
$A+A+e \rightarrow n+A$	$1.4\times10^{-42}\times N_A^2\times(0.026/Te)\times 10^{(100/T0-0.061/Te)}$, $m^6/(s\cdot mol^2)$	third body ionization	-	COMSOL
$e+p \rightarrow A$	$5\times10^{-8}\times N_A$, $m^3/(s\cdot mol)$	recombination	-	COMSOL
$n+p \rightarrow A+A^+$	$2\times10^{-6}\times N_A$, , $m^3/(s\cdot mol)$	recombination	-	COMSOL

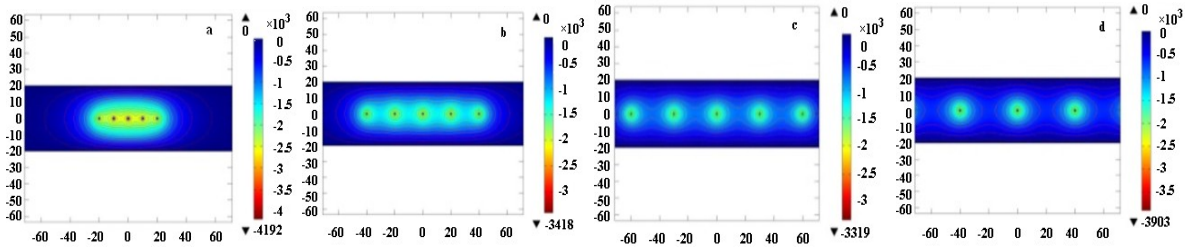

Figure 5. Electric potential distribution with line-line distance for PLP corona discharge: a:10mm; b:20mm; c:30mm; d:40mm.

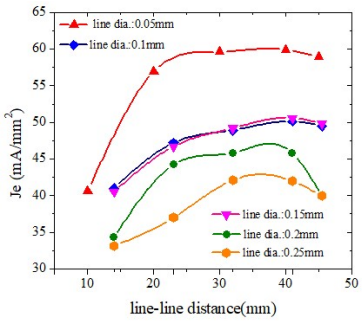

Figure 6. Electric current density of line electrode via line diameter and line-line distance: line-plate distance 20mm and applied voltage 8kV

Figure 7. Experimental setup of PLP negative corona discharge

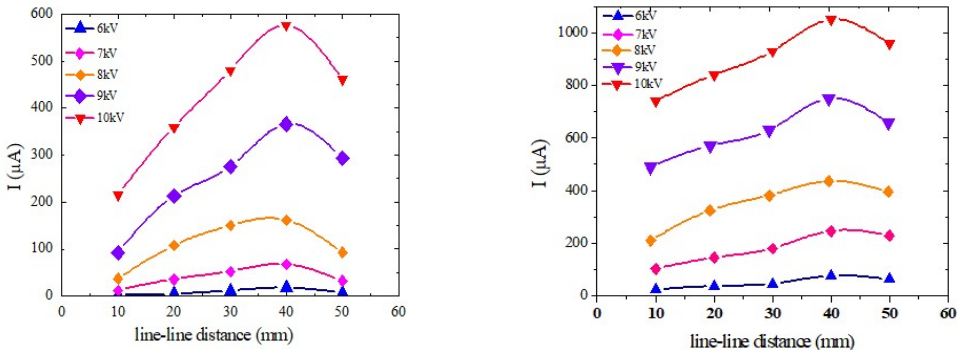

Figure 8. Corona current via line-line distance: line diameter 0.2mm(left) and 0.1mm(right), line-plate distance 20mm

Table 2. Simulation parameters

Parameter	Unit	Value
number of line	-	1-10
line-line distance	mm	10-50
line diameter	mm	0.05-0.3
line-plane distance	mm	10-40
plane length	mm	200-300
plane width	mm	0.001-0.3
gas flow rate	m/s	2.5-3
pressure	MPa	0.1
voltage	kV	1-10

Table 3. Current with line-plate distance: line-line distance 20mm, line diameter 0.2mm, and number of line 5

	Voltage, kV									
Current, μA	1	2	3	4	5	6	7	8	9	10
	line-plate distance 20mm									
	0.02	0.05	0.1	0.15	0.25	3.5	17.5	50	95	160
	line-plate distance 30mm									
	0.01	0.04	0.05	0.1	0.17	0.2	3.7	17	35	57

Table 4. Gas concentrations and removal efficiency

Gas	Initial concentration	Final concentration	Cleaning efficiency, %
Benzaldehyde	2.03 ㎎/㎥	0.170 ㎎/㎥	91.6
Volatile harmful gas	5.36 ㎎/㎥	0.11 ㎎/㎥	97.9
PM2.5	210 ㎍/㎥	15 ㎍/㎥	92.8

Effect of line diameter: The electric current density on the line electrode is investigated by varying the line diameter from 0.05 to 0.25mm and line-line distance from 10 to 50mm, as illustrated in Figure 6. The electric current density is a relevant parameter to estimate the power of corona discharge. In any case, the electric current density is below 65mA/mm^2, which is well accepted for corona discharges. The current density declines with the line diameter, because the electric fieds around the line electrode weakens with the line diameter so the main ion current decreases for the negative PLP corona discharge. The current density grows at the beginning, keeps a plateau and finally declines with the line-line distance. In all case, the threshold line-line distance where the current density drops down, is around 40mm. The reason can be given as follows: the peak electric field and inter-line average potential increase with the line-line distance, while they remain near-constant at over 20 mm. And at over 40mm, the ineter-influnenc of neighbour line electrode can be ignored so that the corona region gets smaller around the line electrode. It can be seen from the fact that the negative coron power could benefit from the lower line diameter and the line-line distance from 20 to 40mm.

Experiments

Setup: In order to verify the simulation result , some experiments were prepared, as shown in Figure 7. The dimensions of aluminium plate electrode are 210 mm long and 120 mm wide, while the length of line electrode is 120 mm. The corona current and voltage are measured by the high-voltage probe Teckatronix PA6015A (1000:1) and oscilloscope Teckatronix DPO4101(1GHz, 5GS/s). A resistance of 50Ω is connected in serial to the discharge circuit and the waveform of current is recorded to the oscilloscope.

Effect of line-plate distance: The corona current was measured by varying the appled voltage from 1 to 10kV with different line-plate distances, as listed in Table 3. As expected in the above simulatition, the corona current lowers with the line-plate distance. It is interesting to mention that the corona current decreases by 2 or 3 times with 1.5 times increase of line-plate distance in all the applied voltage, in spite of some exepections. The corona current gets high with the applied voltage. When the applied voltage is changed between 5 and 8kV, the corona current is significantly increased, which can be regarded as onset of corona discharge. Therefore, the onset volotage of PLP corona discharge increases with the line-plated distance, as well agreed with (7, 9). As a result, the applied voltage should be above 7kV with the line-plate distance of 20mm, and above 8kV with the line-plate distance of 30mm. But the greater the line-plate dstance, the higher applied voltage is requred such that it could lead to some unexpected troubles and dangers. When the line-plate distance is too small, the corona region is also so small that the application may be limited, including gas pressure loss.

Optimized line-line distance: Experiment results indicate that the corona current has a peak around the line-line distance of 40mm, as illustrated in Figure 8. The above simulation also reflects the existence of an optimized line-line distance. The corona current grows with the line-line distance and then finally drops. The tendency of corona current is similar for different voltages and different line diameters. The maximum corona current reflects the largest corona region with high electric field. In our case, the relevant ratio between line-line distance and line-plate distance is therefore decuced to be 1.7 to 2. The above results recommend that the line-line distance should be double the line-plate distance in order to form a stable corona discharge under different voltages, air pressures, numbers of line electrodes, line diamters and line-plate distance. It can be seen that an optimized line-line distance exists with a given line-plate distance. The reason is as follows: if the line-line distance gets smaller, the electric field becomes lower than in a line electrode because of interaction of neighboured line electrodes, and therefore electron emission gets weaker as the corona current drops down. If the number of line increases, it appears closer in relative to the plate electrode, thereby decreasing the electric field around the line electrodes. And, in order to obtain a high corona current by strengthening the electron emission, surface area of the line should be increased, but too large surface area degrades the current density and the electric field gets weaker. It can be concluded from experiment and simulation resutls that the optimized ratio of line-line distance and line-plate distance should be 1.7-2.0 for the PLP negative corona discharge.

CONCLUSION

We performed simulations and experiments of PLP negative corona discharge and estimated its optimized electrode arrangement. The line-plate distance was varied from 10mm to 30mm and the line-line distance from 10 to 50mm. The results showed that the optimized line-line and line-plated distances are 34 to 40mm and 20mm, when the corona current, peak electric field, inter-line average potential, and corona region become the largest. So it is suggested that the relevant ratio between line-line and line-plate distances is 1.7-2.0. Our PLP negative corona discharge was applied to removal of harmful gases. The main harmful gases in the workshop were tri-ethanolamine, benzaldehyde, acetone, and acrylic butyl. The bad smell comes mainly from acrylic butyl in UV coating solution. The emission of acrylic butyl was 0.145㎏ per hour and its acceptable level is 0.01㎎/m^3. In order to assess the removal performance of the harmful gases, the gas contaminations in the workshop were measured by a gas meter MEF550. After 30 min removal processing, the removal performance was estimated, as listed in table 4. It was found that the removal efficiency of benzaldehyde is 91.6%, 97.9% for volatile harmful gas ,and 92.8% for PM2.5 dust particle.

REFERENCES

Toshiaki, et al., Plasma Electronics, Applications in Microelectronic Device Fabrication, CRC Press, Taylor & Francis Group, 2015: 100-228.

Rong M, Liu D, Wang D, Su B, Wang X, Wu Y, A New Structure Optimization Method for the Interneedle Distance of a Multineedle-to-Plane Barrier Discharge Reactor, IEEE Trans. Plasma Sci., 2010; 38(4): 966-972.

Zakari M, et al. An axisymmetric unstructured finite volume method applied to the numerical modeling of an atmospheric pressure gas discharge, J. Comput. Phys., 2015; 281: 473-492.

Fukui T, Masuno K, Makita Y, Fujiwara S, Shiota G., Imamura Y, Shiba A, Wang PL, Evaluation of oral mucosa irritation produced by ozone gel, J. hard tissue diology. 2015; 24 (1): 104-106.

Zheng Y, He J, Zhang B, Li W, Zeng R, Ion Flow Effects on Negative Direct Current Corona in Air, Plasma Chem. Plasma Process. 2010; 30: 55-73.

Cheng G, Chen Y S, Hwang F N, Wu J S, Hung C T, Hu M H, Lin K M, A parallel hybrid numerical algorithm for simulating gas flow and gas discharge of an atmospheric pressure plasma jet, Comp. Phys. Comm., 2012; 183: 2550-2560.

Michael G., Deng X T, Electrically efficient production of a diffuse nonthermal atmospheric plasma, IEEE Trans. Plasma Sci. 2003; 31 (1): 7-18.

Paria S, Peter C G S, Adamiak K, Numerical Simulation of Trichel Pulses in a Negative Corona Discharge in Air, IEEE Trans. Ind. Appl. 2011; 47 (4): 1935-1941.

Kenneth L K, Electrostatic Discharge ,CRC Press, Taylor & Francis Group , LLC, 2006: 1-102.

Zhao L, Adamiak K, Numerical Simulation of the Electrohydrodynamic Flow in a Single Wire-Plate Electrostatic Precipitator, IEEE Trans. Ind. Appl. 2008; 44 (3): 683-690.

Papageorgiou L, Metaxas A C, Georghiou G E, Three-dimensional numerical modelling of gas discharges at atmospheric pressure incorporating photoionization phenomena, J. Phys. D, Appl. Phys. 2011; 44: 045203.

Papageorgiou L, Metaxas A C, Georghiou G E, Three-dimensional streamer modeling in atmospheric pressure air, IEEE Trans. Plasma Sci. 2011; 39(11): 2224-2225.

Breden D, Miki K, Raja L L, Self-consistent two-dimensional modeling of cold atmospheric pressure plasma jets/bullets, Plasma Sources Sci. Technol. 2012; 21 (3): 034011.

Benkhaldoun F, Fořt J, Hassouni K, Karel J, Simulation of planar ionization wave front propagation on an unstructured adaptive grid, J. Comput. Appl. Math. 2012; 236: 4623-4634.

Sato T, Hasegawa T, Fue H, Mukaigawa S, Takaki K, Fujiwara T, Self-organization pattern of microgap atmospheric barrier discharge, IEEE Trans. Plasma Sci. 2011; 39 (11): 2202-2203.

Tanaka S, Horinouchi T, Abe S, Matsuno Y, Sasaki T, Kikuchi T, Harada N, Inactivation Property of Microorganisms in Water Irradiated by Atmospheric-Pressure Plasma using Dielectric Barrier Discharge, IEEJ Trans. Electrical and Electronic Engineer, 2013; 8: 105-110.

Payen E, Dubruel P, Frère-Trentesaux M, Van Vlierberghe S, Morent R, De Geyter N, Effect of electrode geometry on the uniformity of plasma-polymerized methyl methacrylate coatings, Prog. Org. Coating. 2011; 70(4): 293-299.

Wang X, Sun C, Formation conditions for transported charges of multineedle-to-cylinder dielectric barrier discharge based on the orthogonal design and lissajous figures, in: Int. Conf. on Inform. Sci. and Eng. Application. 2011: 21-23.

Bahaeva N Y, Kushner M J, Intracellular electric fields produced by dielectric barrier discharge treatment of skin, J. Phys. D: Appl. Phys. 2010; 43: 185-206.

Shao X J, Zhang G J, Ma Y, Li Y X, One-dimensional modeling of dielectric barrier discharge in xenon, IEEE Trans. Plasma Sci. 2011; 39 (4): 1165-1172.

Pien F, Zainuddin N S, Ha H L, Dayou J, Analysis and characterization of enhanced kinetic reaction on ozone generation using negative corona discharge, J. Phys. Commun. 2020; 4: 075022.

Dai Y, Zhang Z, Dong Z, Wu Y, Jun D, Research on Ultraviolet Characteristics Parameters of DC-Positive Polarity Corona Discharge on Conductors, Appl. Sci. 2024; 14: 3258.

Leng J, Liu Z, Zhang X, Huang D, Qi M, Yan X, Design and analysis of a corona motor with a novel multi-stage structure, J. Electrost. 2021; 109: 103538.

Wang J, Zhu T, Cai Y X, Zhang J F., Wang J B, Review on the recent development of corona wind and its application in heat transfer enhancement, Int. J. Heat Transfer, 2020; 152: 119545.

Liu P, Song Y, Zhang Z, A Novel Dielectric Barrier Discharge (DBD) Reactor with Streamer and Glow Corona Discharge for Improved Ozone Generation at Atmospheric Pressure, Micromechanics, 2021; 21: 1287.

Arcanjo M, Monranya J, Urbani M., Lorenzo V., Pineda N., Observations of corona point discharges from grounded rods under thunderstorms, Atmos. Res. 2021; 247: 105238.

****